FULL PAPERS

Magnetic Resonance in Medicine 59:959–965 (2008)

Toward Improved Grading of Malignancy in Oligodendrogliomas Using Metabolomics

G. Erb,[1,2] K. Elbayed,[2] M. Piotto,[2,3] J. Raya,[2] A. Neuville,[4] M. Mohr,[4] D. Maitrot,[5] P. Kehrli,[5] and I.J. Namer[1*]

In spite of having been the object of considerable attention, the histopathological grading of oligodendrogliomas is still controversial. The determination of reliable biomarkers capable of improving the malignancy grading remains an essential step in working toward better therapeutic management of patients. Therefore the metabolome of 34 human brain biopsies, histopathologically classified as low-grade (LGO, *N* = 10) and high-grade (HGO, *N* = 24) oligodendrogliomas, was studied using high-resolution magic angle spinning nuclear magnetic resonance spectroscopy (HRMAS NMR) and multivariate statistical analysis. The classification model obtained afforded a clear distinction between LGOs and HGOs and provided some useful insights into the different metabolic pathways that underlie malignancy grading. The analysis of the most discriminant metabolites in the model revealed the presence of tumoral hypoxia in HGOs. The statistical model was then used to study biopsy samples that were classified as intermediate oligodendrogliomas (*N* = 6) and glioblastomas (GBMs) (*N* = 30) by histopathology. The results revealed a gradient of tumoral hypoxia increasing in the following direction: LGOs, intermediate oligodendrogliomas, HGOs, and GBMs. Moreover upon analysis of the clinical evolution of the patients, the metabolic classification seems to provide a closer correlation with the actual patient evolution than the histopathological analysis. Magn Reson Med 59:959–965, 2008. © 2008 Wiley-Liss, Inc.

Key words: oligodendroglioma; glioblastoma; MR spectroscopy; high-resolution magic angle spinning nuclear magnetic resonance (HRMAS NMR); metabolics

Oligodendrogliomas represent 5% to 18% of adult gliomas and their clinical management is known to differ from other gliomas, especially regarding their sensitivity to radio- and chemotherapy (1). Most oligodendrogliomas grow slowly but inevitably evolve into a malignant form. The histopathological diagnosis of oligodendrogliomas and the correct grading of their malignancy are crucial steps to establish an accurate prognosis and to define the optimum surgical and therapeutic strategies, since they may trigger or delay radio- and chemotherapy. However, at the present time, the search for specific biomarkers to identify oligodendrogliomas has not yet been successful (2,3). Despite improvements in the malignancy grading systems, no consensus has yet been found as to which morphological features constitute unambiguous criteria of malignancy (1,4–7). Using existing classifications methods, it is common to observe, on one hand, tumors classified as low-grade oligodendrogliomas (LGOs) with poor evolution and, on the other hand, tumor classified as high-grade oligodendrogliomas (HGOs) with relatively long survival time. These disagreements between the malignancy grading and the prognosis should be overcome. Therefore the determination of reliable biomarkers, such as 1p/19q loss, related to patient prognosis is essential for better therapeutic management of patients (8–10).

Metabolomic analysis aims at quantifying and identifying all metabolites in an organ or a tissue, at the cellular or even at the subcellular level (11–13). For most purposes, it is not necessary to quantify the absolute amounts of metabolites but only their relative ratios in pathologic and healthy situation. Metabolomic analyses result in the detection of almost 50 different metabolites in brain biopsies (14–19). In order to gain meaningful biological information from metabolic profiles, it is necessary to evaluate the data both statistically and bioinformatically to gain information on the underlying metabolic pathways via known or calculated biochemical networks (20,21).

PATIENTS AND METHODS

Patients

In this prospective study, 34 patients, histopathologically classified as LGOs (10 patients, seven men and three women; mean age = 48.5 ± 19.6 years) and HGOs (24 patients, 17 men and seven women; mean age = 44.6 ± 12.0 years), respectively, with grade II and III in the World Health Organization (WHO) classification, were studied. To evaluate the predictive properties of this statistical model, six intermediate cases of oligodendrogliomas (WHO grade II/III; five men and one woman; mean age = 37.7 ± 14.2 years) and 30 histopathologically classified glioblastomas (GBMs, WHO grade IV; 12 men and 18 women; mean age = 51.3 ± 19.6 years) were also included. The clinical follow-up of all the 70 patients was monitored using ^{1}H-MRSI (at 3-month intervals) and MRI (at 6-month intervals).

[1]Department of Biophysics and Nuclear Medicine, University Hospitals of Strasbourg, France

[2]Université Louis Pasteur (ULP)/Centre National de la Recherche Scientifique (CNRS) LC3-Unité Mixte de Recherche (UMR) 7177, Strasbourg, France

[3]Bruker Biospin, Wissembourg, France

[4]Department of Pathology, University Hospitals of Strasbourg, Strasbourg, France

[5]Department of Neurosurgery, University Hospitals of Strasbourg, Strasbourg, France

Grant sponsors: Bruker Biospin; Université Louis Pasteur (ULP); Hôpitaux Universitaires de Strasbourg; PHRC-03.

*Correspondence to: I.J. Namer, Department of Biophysics and Nuclear Medicine, University Hospitals of Strasbourg, Avenue Moliere, Strasbourg, 67000, France. E-mail: Izzie.Jacques.NAMER@chru-strasbourg.fr

Received 4 April 2007; revised 22 October 2007; accepted 24 October 2007.

DOI 10.1002/mrm.21486

Published online in Wiley InterScience (www.interscience.wiley.com).

Sample Collection and Preparation

Resected tissue specimens were collected immediately after patient operation and were snap-frozen in liquid nitrogen before being stored at −80°C. For the high-resolution magic angle spinning (HRMAS) analysis, the amount of tumoral tissue used ranged from 12 to 40 mg. Each sample was introduced into a 4-mm ZrO_2 rotor fitted with a 50-μl cylindrical insert. A total of 10 μl of D_2O were then added to the rotor to provide a lock frequency for the nuclear magnetic resonance (NMR) spectrometer. The exact weight of sample was determined by weighing the empty rotor and the rotor containing the biopsy. The rotor was stored back at −80°C until the time of HRMAS analysis. Before inserting the rotor into the NMR probe, the probe was precooled to 3°C. The whole HRMAS study was performed at 3°C and started immediately after the temperature inside the probe reached the equilibrium condition (5 min).

HRMAS NMR

HRMAS spectra were recorded on a Bruker Avance 500 spectrometer operating at a proton frequency of 500.13 MHz. The instrument was equipped with a 4-mm triple resonance (^1H, ^{13}C, ^{15}N) gradient HRMAS probe. A Bruker Cooling Unit (BCU) was used to keep the sample temperature at 3°C. For all NMR experiments, samples were spun at 3 kHz in order to keep the rotation sidebands out of the spectral region of interest. One-dimensional (1D) ^1H spectra using water presaturation were acquired in 32 min and 128 scans. For each sample, spectra were also acquired using a Carr-Purcell-Meiboom-Gill (CPMG) pulse sequence in order to attenuate the broader signals arising from the macromolecular tissue components such as the lipoproteins, thereby giving a clearer representation of the lower molecular weight components. 1D ^1H CPMG spectra were acquired using the following pulse sequence (relaxation delay 90°–$(\tau–180°–\tau)_n$– acquire FID) with $N = 40$ and using 128 transients. To decrease the effects of radio frequency field inhomogeneities (22,23) the CPMG pulses were synchronized with the sample spinning (τ = 333.33 μs). To assign all the resonances, 2D homonuclear ^1H-^1H and heteronuclear ^1H-^{13}C experiments were recorded on three samples. 2D ^1H-^1H J-correlation spectra using a decoupling in the presence of scalar interactions (DIPSI)-2 mixing sequence were acquired with a 170-ms acquisition time, a 50-ms mixing time, a 6000-Hz spectral width, and a 1.5-s relaxation delay. A total of 16 transients were averaged for each of the 256 increments during t1, corresponding to a total acquisition time of 2 h. 2D ^1H-^{13}C gradient heteronuclear single quantum correlation (g-HSQC) (24) experiments were acquired using a 170-ms acquisition time with globally optimized alternating phase rectangular pulse (GARP) ^{13}C decoupling and a 1-s relaxation delay. A total of 256 transients were averaged for each of 256 t1 increments, corresponding to a total acquisition time of 21 h. To detect a possible degradation of the sample during the course of the NMR experiments, a control experiment consisting of a 1D ^1H HRMAS spectrum was recorded before and after each set of experiments and no metabolite degradation was detected. As a further proof of sample stability under the experimental conditions used, 1D ^1H spectra were recorded at 3°C on three different samples every hour during a 24-h period and no evolution of the spectra was observed.

Statistical Analysis

1D HRMAS NMR spectra were data reduced into 200 integral regions of 0.02 ppm width between 4.5 and 0.5 ppm using the software program AMIX (Analysis of MIXtures version 2.5; Bruker Rheinstetten, Germany) and exported into SIMCA P (version 11.0; Umetrics AB, Umeå, Sweden) where partial least square discriminant analysis (PLS-DA) was conducted. All analyses used Pareto scaling (scaling factor $1/\sqrt{SD}$) to accommodate the influence of metabolites present in both high and low concentrations in the model, but without emphasizing spectral noise. PLS-DA is a supervised analysis procedure (i.e., a method incorporating prior knowledge of class identity) that tries to maximize the separation between classes, rather than explaining the maximum variation in the data, or to construct statistical boundaries around each class.

PLS-DA was performed on the data to obtain a metabolic description of each oligodendroglioma type. To test the resulting supervised models, the class membership of every sample was iteratively predicted and the results were used to generate a measure of the goodness of the fit (Q^2) for the overall model. The theoretical maximum is 1 for a perfect prediction. In order for a PLS component to be considered significant, Q^2 must be significantly larger than zero and is generally considered as good when equal or superior to 0.5. This technique provides predictive capability and was used to model spectral changes in terms of metabolites variations. While Q^2 is related to the predictive power of the model for each data set, the predictive capability of the model was also calculated directly and represented as a percentage of success rate if the score/disease status was specified within a given limit (25,26).

The resulting statistical model can then be used to classify unknown samples and attribute them to a specific class of the model. Interpretation of the regression coefficients provides information on the most discriminant metabolites used in the model and gives some insight into the metabolic pathways involved.

RESULTS AND DISCUSSION

In this work, we have used a metabolomic approach in order to gain some insights into the mechanisms of increasing malignancy at the molecular level. Metabolomics is an elegant way to bridge the gap between clinical prognosis and the grading system. A total of 34 patients, histopathologically classified as follows: 10 LGOs (seven men and three women; mean age = 48.5 ± 19.6) and 24 HGOs (17 men and seven women; mean age = 44.6 ± 12.0), grade II and III in the WHO classification, respectively, were studied. Each sample was studied using HRMAS NMR spectroscopy, a technique that has recently demonstrated its potential for analyzing intact biological tissues (Fig. 1). To interpret this global metabolic information, the data were subjected to a multivariate statistical analysis using a supervised analysis procedure that makes use of the primary histological classification (LGO vs. HGO). The re-

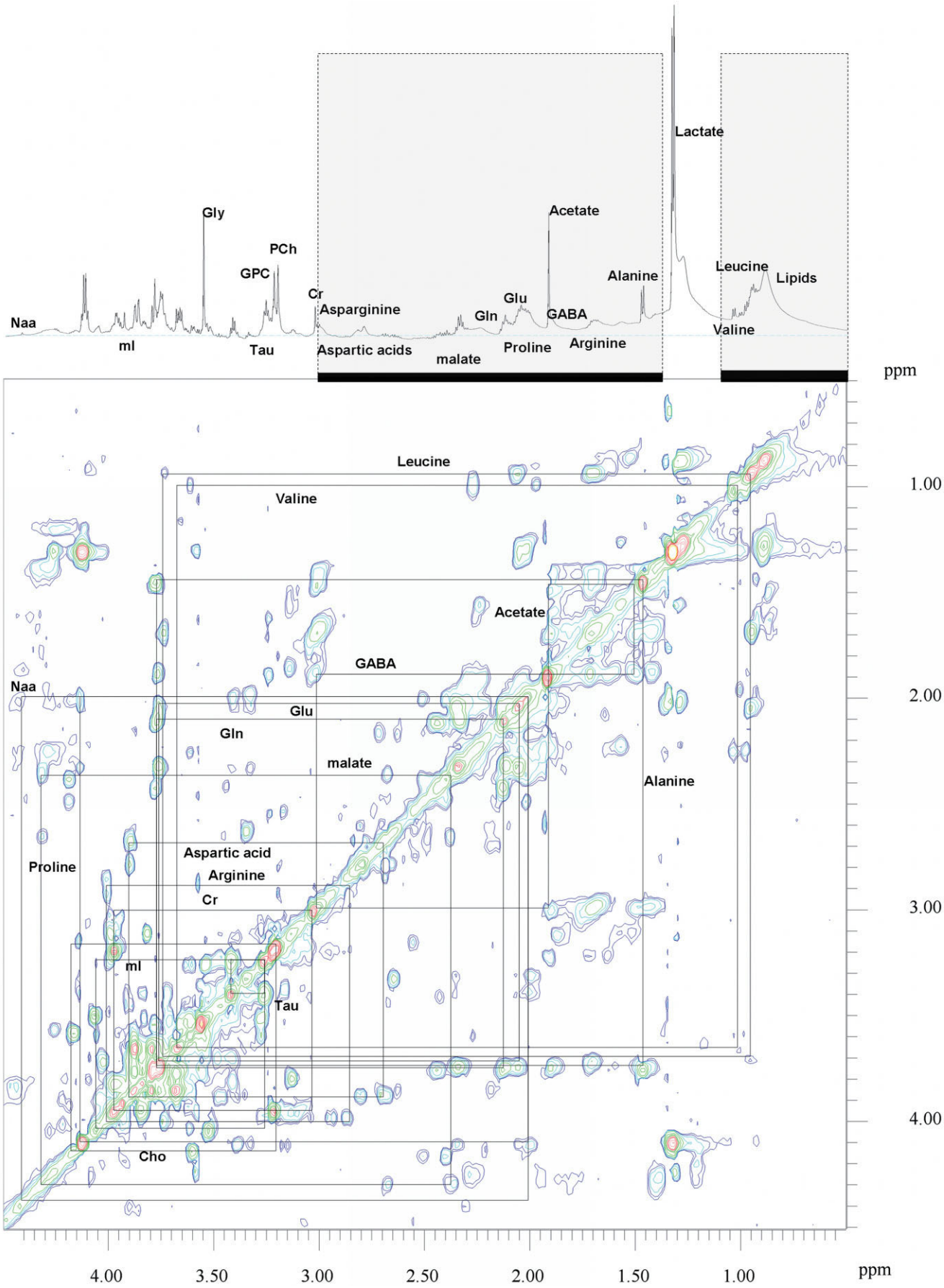

FIG. 1. 1D ^{1}H and 2D total correlation spectroscopy (TOCSY) HRMAS spectra of a brain tumor sample from a patient diagnosed as HGO. Partial metabolite assignments in the 4.5 to 0.5 ppm region are shown. The underlined part of the 1D spectrum corresponds to the spectral region used in the amino acid metabolism analysis. [Color figure can be viewed in the online issue, which is available at http://www.interscience.wiley.com.]

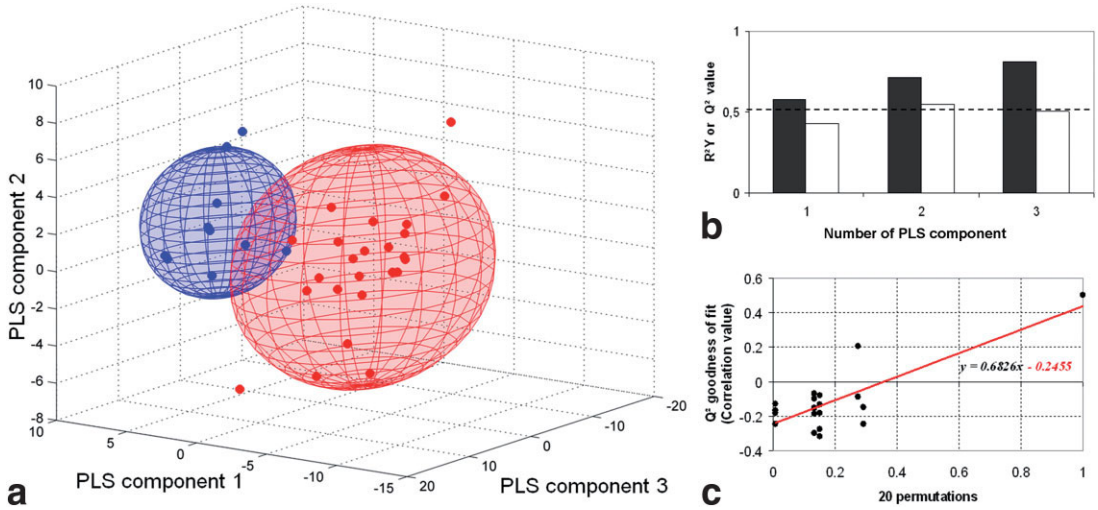

FIG. 2. Global spectral analysis. **a:** 3D plot showing the first three component of the PLS-DA computed on histopathologically classified LGOs (blue points) and HGOs (red points). The 95% confidence criteria volume (1.96 × SD) for each group is represented. This model allows a clear separation, with only a small overlap of the LGO and HGO spatial distribution. **b:** PLS-DA is validated by a cumulative R^2Y (black bar) equal to 0.81. The cumulative Q^2 (white bar) value obtained for three components, which is equal to 0.5, indicates a good predictivity for the model. **c:** Correlation coefficient between the original Y (histopathological classification hypothesis) and the permuted Y vs. the cumulative Q^2 represented by a regression line whose value is negative at the origin. This feature demonstrates that there is no overfit of the model.

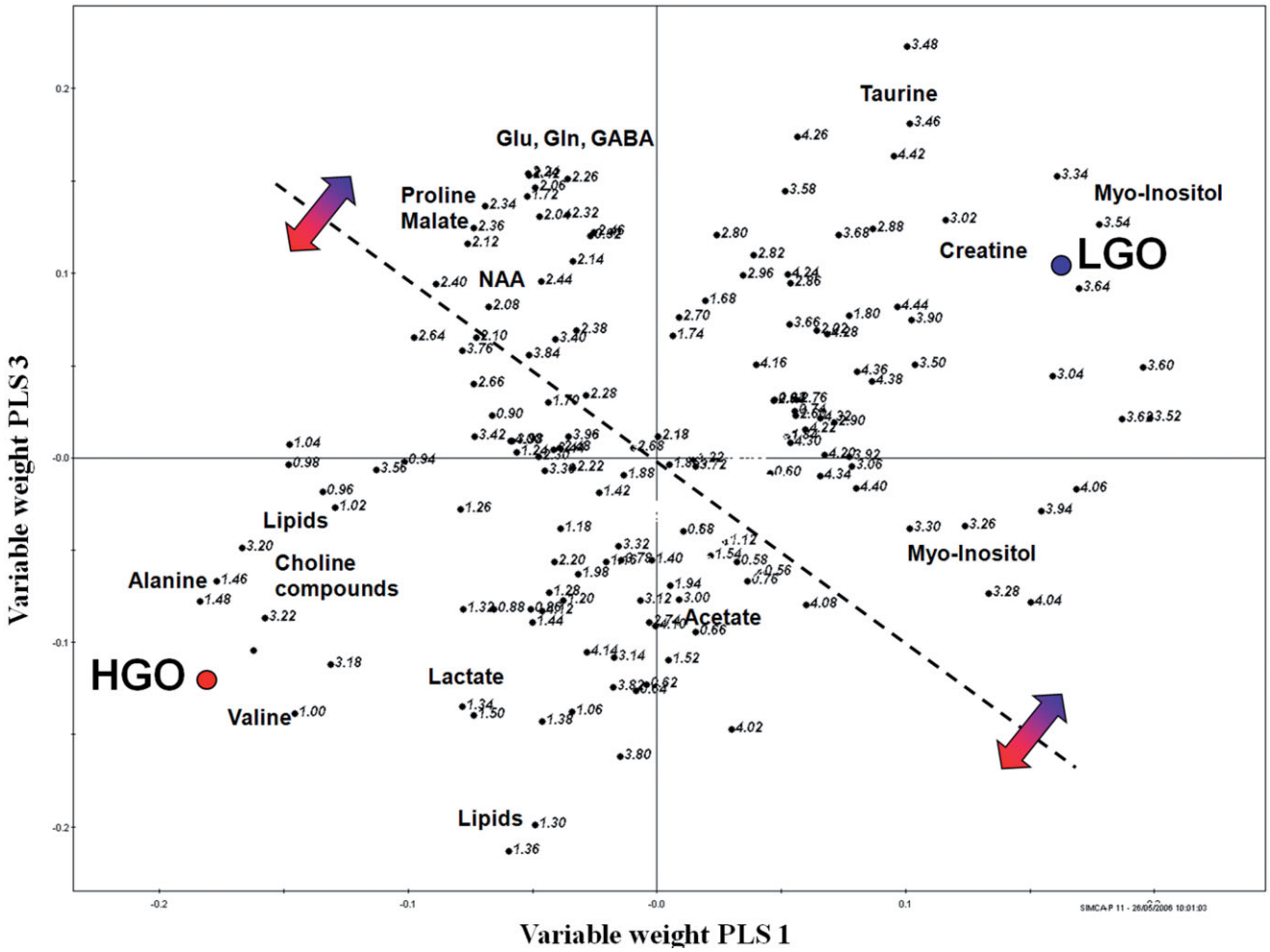

FIG. 3. Global variable weights in oligodendroglioma classification: Plot of PLS-DA weights showing the first and third components for LGOs (blue) vs. HGOs (red) classification. Each point (numerical value in ppm) represents a single bucket (i.e., 0.2-ppm interval in the HRMAS NMR spectra), which is correlated to one or several metabolites. Most valuable buckets underlying this classification are displayed in the figure: alanine, lipids, valine, the total choline compounds, proline, myoinositol, taurine, glutamine (Gln), glutamate (Glu), GABA, NAA, acetate, and creatine. Differences between LGOs and HGOs are given in terms of bucket weights in PLS components computation.

sponse variable set (Y-data) was created by indicating the classes of observations (LGO vs. HGO) in the training set and a PLS-DA model was fitted to the training set (200 variables per observation) X-matrices. PLS analysis is probably the least restrictive of the various multivariate extensions of the multiple linear regression models. Its flexibility allows it to be used for situations in which the use of traditional multivariate methods is severely limited, such as the case when there are fewer observations than predictor variables (21). This technique is a powerful tool that defines automatically the combination of metabolic variables that best describe the clustering in malignancy grading.

The results obtained using PLS-DA show a clear separation between LGOs and HGOs on the basis of the whole set of metabolic variables. The model generated with three significant PLS-components (determined by cross validation) had a cumulative fit to the Y-data (R2Y) of 0.82 and a cumulative confidence criterion of prediction of 0.50 (Q^2) (Fig. 2). As the number of observations is limited, cross-validation was performed by first excluding a portion of the available data from the model training and then by predicting their classification using the model. This process was repeated until all the data were left out once. In our case, each patient was kept out of the model development and then classified using the model. This procedure was repeated for the whole series of patients and no misclassification of the LGO or HGO population was detected.

Although the direct identification of the metabolites is not necessary to achieve the classification, analyzing the different metabolites at the origin of the classification can lead to the detection of pathological biomarkers and to a better understanding of the tumoral metabolism. The most discriminant metabolites contributing to the model were found to be: alanine, lipids, valine, total choline compounds, proline, myoinositol, taurine, glutamine, glutamate, γ-aminobutyric acid (GABA), malate, N-acetyl-aspartate (NAA), acetate, and creatine (Fig. 3). In agreement with several publications discussing the fixation of fluorodeoxy-D-glucose in gliomas (27), our results show that glucose is not a discriminating biomarker between LGOs and HGOs. The lactate concentration or the total amount of amino acids detected by HRMAS is also not statistically different between LGOs and HGOs. What is however clear is that HGOs show an increase of amino acid production via nonoxidative pathways, indicating that the energy metabolism shifts toward fermentative metabolism when the oligodendrogliomas evolve from a LGO to a HGO (28–30).

We then computed a new model focussed on the amino acid metabolism. This model included the most valuable metabolites described by the global model but excluded choline compounds (membrane turnover), myoinositol (glial metabolism), and creatine. To reduce the contribution of lipid signals that may obscure metabolite resonances, the model was built using the spectra resulting from a CPMG HRMAS experiment. The CPMG sequence is known for its ability to attenuate the contribution from molecules with a short T_2 relaxation time (i.e., the lipids). Using only the metabolites related to the amino acid metabolism (Fig. 1) with the goal of probing oxidative vs. nonoxidative amino acids production pathways, the metabolic clustering of LGO and HGO was maintained (Fig. 4): the model generated with four significant PLS-components had a cumulative fit to the Y-data (R2Y) of 0.82 and a cumulative confidence criteria of prediction of 0.46 (Q^2), with only one HGO misclassified. As in the previous case, the classification was validated by circular validation.

As the model generated from the partial metabolic dataset had a cumulative fit to the Y-data and a cumulative confidence criteria of prediction similar to the one gener-

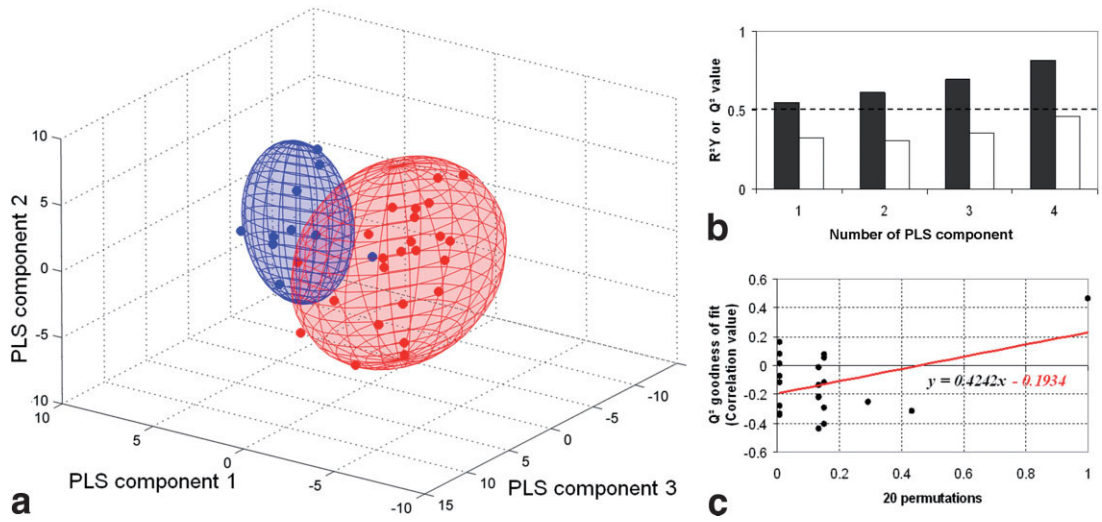

FIG. 4. Amino acid metabolism analysis. **a:** 3D plot showing the first three component of the PLS-DA computed using histopathologically-classified LGOs (blue points) and HGOs (red points) using only the NMR spectral region corresponding to the amino acid metabolism. The 95% confidence criteria volume (1.96 × SD) for each group is represented. An efficient separation is also well achieved with this model, with only a small overlap of the LGO and the HGO spatial distribution. **b:** PLS-DA is validated by a cumulative R^2Y (black bar) equal to 0.81. The cumulative Q^2 (white bar) value is close to 0.5 and indicates a good predictability for the model. **c:** Correlation coefficient between the original Y (histopathological classification hypothesis) and the permuted Y vs. the cumulative Q^2 represented by a regression line whose value is negative at the origin. This feature demonstrates that there is no overfit of the model.

ated using the full metabolite set, it became clear that the distinction between LGOs and HGOs is principally due to the metabolites involved in amino acid metabolism. We observed that in HGO the alanine and the valine production, which are related to the anaerobic pathway, are increased whereas proline, glutamate, glutamine, GABA, and NAA, which are related to the Krebs pathway, are decreased. This metabolic shift toward fermentative metabolism clearly reflects tumor hypoxia in HGOs. Including information pertaining to the lipids, the choline compounds and myoinositol only slightly improved the classification.

To evaluate the predictive properties of this statistical model, six intermediate cases of oligodendrogliomas (WHO grade II/III; five men and one woman; mean age = 37.7 ± 14.2 years) and 30 histopathologically classified GBMs (WHO grade IV; 12 men and 18 women; mean age = 51.3 ± 19.6 years) were studied by metabolomics. The results revealed that the classification reflects a gradient of hypoxia increasing in the following direction: LGOs, HGOs, and GBMs . The intermediate grade II/III oligodendrogliomas cases occur, either in the LGO region or in the border region between LGO and HGO (Fig. 5). A closer inspection of the data reveals that the metabolic model is not perfectly correlated with the histopathological grading. The classification obtained using the metabolic analysis probably reflects complex metabolic processes that correlate better with the patient's clinical course. Almost all GBMs have poor prognosis (survival time = 11 ± 9 months) and our metabolomic model reflects this fact by regrouping them on one extremity of the metabolic distribution. However, some GBM cases that are detected as metabolically close to HGOs or LGOs display a relative long survival time (22 ± 9 months). In the same way,

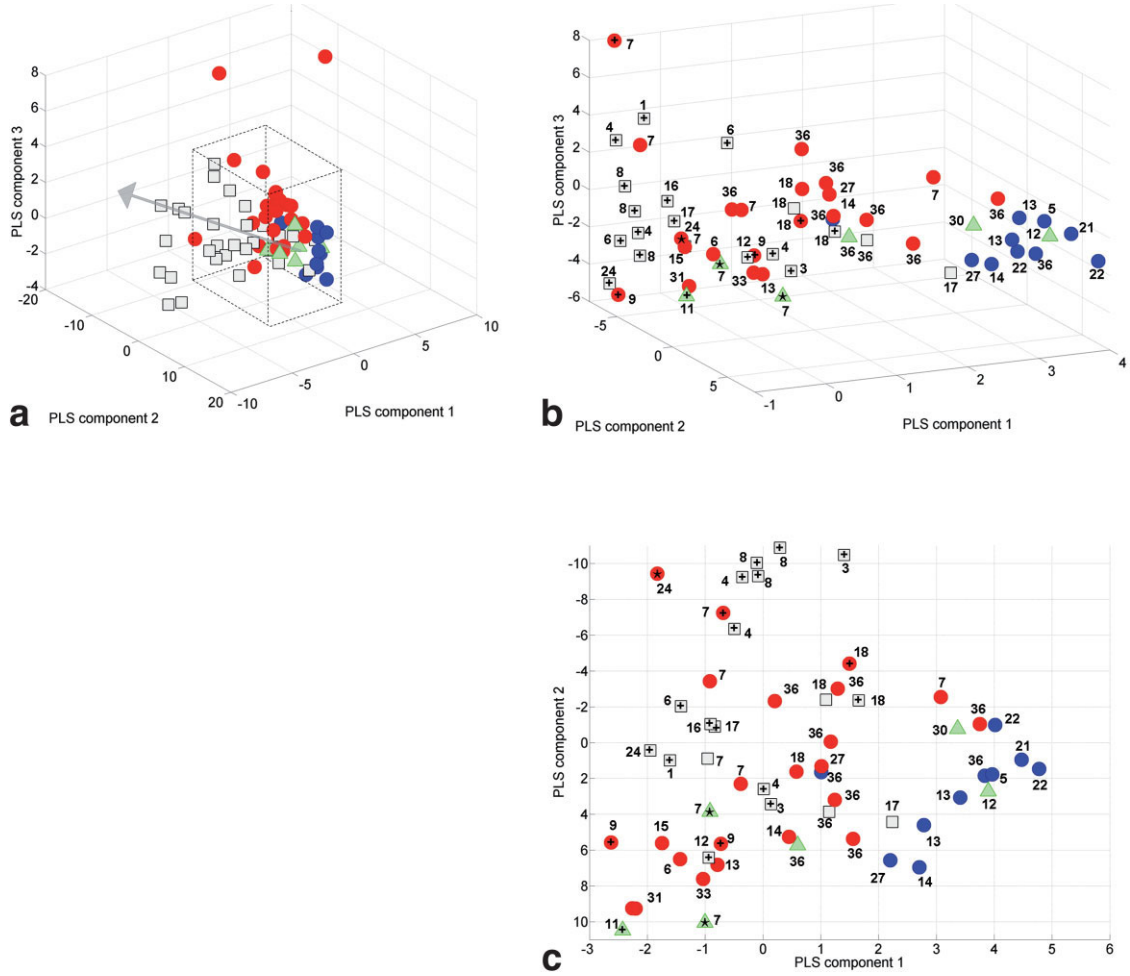

FIG. 5. Application of the statistical model to new histopathologically classified cases. **a:** 3D plot showing the first three components of the PLS-DA model computed with LGOs (blue dots) and HGOs (red dots) using only the NMR spectral region corresponding to the amino acid metabolism. Introduction of intermediate oligodendrogliomas (green triangles) and GBM cases (black squares) in the model shows a metabolic shift reflecting roughly the histopathological malignancy grading: LGOs (WHO grade II), intermediate cases of oligodendrogliomas (WHO grade II/III), HGOs (WHO grade III), and GBMs (WHO grade IV). The arrow indicates the apparent direction from the barycenter of the LGO distribution to the barycenter of the GBM distribution and corresponds to an increase in malignancy. **b**,**c:** Focusing on the overlapping region of the four groups (dashed box on Fig. 5a), we observe that the metabolomic classification seems to be better correlated to the clinical evolution than the histopathological grading. The numbers indicate the time elapsed (in months) since the initial diagnosis. Patient death is represented by (+) and tumor recurrence by (★).

intermediate oligodendroglioma cases present heterogeneous metabolic pattern correlated with clinical evolution: three cases that are metabolically close to HGOs and GBMs present bad prognosis with a very short recurrence period (7 months in two cases, and death after 11 months for the third one) and the three other cases close to LGOs present better prognosis (no tumor progression during clinical screening elapsed time, from 12 to 36 months).

CONCLUSIONS

The significance of the histopathological diagnosis is based largely on its ability to predict prognosis and its ability to predict the patient's response to different treatment modalities. However, in the case of gliomas, morphologic criteria are probably insufficient. The present findings suggest that the metabolic information (the degree of tumor hypoxia) obtained at an early state of disease could be better correlated with the patient prognosis than the morphological criteria (28–30). This property should allow us to better understand variable clinical evolution and atypical cases. Moreover, the diagnosis of hypoxia is of direct clinical relevance to the successful treatment of cancer, in particular hypoxia in tumors can affect the outcome of chemotherapy and radiotherapy treatments.

In spite of the relatively short screening period of the patients (3 years), our observations suggest that a metabolomic study, associated with histopathology and molecular biology data, could become a reliable indicator of patient prognosis. Metabolomic data acquired on a larger population could therefore become an essential element for a better therapeutic management of the patient.

ACKNOWLEDGMENTS

The technical assistance of Mrs. F. Ackermann in preparing the tumor samples is gratefully acknowledged. We also thank Dr. R. Kannan-Piotto for proofreading the manuscript. This study was approved by the Alsace Ethics Committee (no. 03/100, 09.12.2003).

REFERENCES

1. Kleihues P, Cavenee WK. WHO international histopathological classification of CNS tumors. Pathology and genetics tumors of the nervous system. Lyon: IARC; 2000. p. 55–70.
2. Hoang-Xuan K, Aguirre-Cruz L, Mokhtari K, Marie Y, Sanson M. OLIG-1 and 2 gene expression and oligodendroglial tumours. Neuropathol Appl Neurobiol 2002;28:89–94.
3. Burger P, Scheithauer B. Oligodendroglial neoplasms. Atlas of tumor pathology, Series 3, Fascicle 10. Washington, DC: Armed Forces Institute of Pathology; 1994. p 107–120.
4. Earnest F III, Kernohan JW, Craig WM. Oligodendrogliomas; a review of 200 cases. Arch Neurol Psychiatry 1950;63:964–976.
5. Smith MT, Ludwig CL, Godfrey AD, Armbrustmacher VW. Grading of oligodendrogliomas. Cancer 1983;52:2107–2114.
6. Shaw EG, Scheithauer BW, O'Fallon JR, Tazelaar HD, Davis DH. Oligodendrogliomas: the Mayo Clinic experience. J Neurosurg 1992;76:428–434.
7. Daumas-Duport C, Tucker ML, Kolles H, Cervera P, Beuvon F, Varlet P, Udo N, Koziak M, Chodkiewicz JP. Oligodendrogliomas. Part II: a new grading system based on morphological and imaging criteria. J Neurooncol 1997;34:61–78.
8. Sanson M, Thillet J, Hoang-Xuan K. Molecular changes in gliomas. Curr Opin Oncol 2004;16:607–613.
9. Reifenberger J, Reifenberger G, Liu L, James CD, Wechsler W, Collins VP. Molecular genetic analysis of oligodendroglial tumors shows preferential allelic deletions on 19q and 1p. Am J Pathol 1994;145:1175–1190.
10. Louis DN, Holland EC, Cairncross JG. Glioma classification: a molecular reappraisal. Am J Pathol 2001;159:779–786.
11. Nicholson JK, Lindon JC, Holmes E. "Metabonomics": understanding the metabolic responses of living systems to pathophysiological stimuli via multivariate statistical analysis of biological NMR spectroscopic data. Xenobiotica 1999;29:1181–1189.
12. Fiehn O. Metabolomics—the link between genotypes and phenotypes. Plant Mol Biol 2002;48:155–171.
13. Griffin JL, Shockcor JP. Metabolic profiles of cancer cells. Nat Rev Cancer 2004;4:551–561.
14. Griffin JL. Metabonomics: NMR spectroscopy and pattern recognition analysis of body fluids and tissues for characterisation of xenobiotic toxicity and disease diagnosis. Curr Opin Chem Biol 2003;7:648–654.
15. Martinez-Bisbal MC, Marti-Bonmati L, Piquer J, Revert A, Ferrer P, Llacer JL, Piotto M, Assemat O, Celda B. 1H and 13C HR-MAS spectroscopy of intact biopsy samples ex vivo and in vivo 1H MRS study of human high grade gliomas. NMR Biomed 2004;17:191–205.
16. Cheng LL, Chang IW, Louis DN, Gonzalez RG. Correlation of high-resolution magic angle spinning proton magnetic resonance spectroscopy with histopathology of intact human brain tumor specimens. Cancer Res 1998;58:1825–1832.
17. Cheng LL, Anthony DC, Comite AR, Black PM, Tzika AA, Gonzalez RG. Quantification of microheterogeneity in glioblastoma multiforme with ex vivo high-resolution magic-angle spinning (HRMAS) proton magnetic resonance spectroscopy. Neuro Oncol 2000;2:87–95.
18. Lehnhardt FG, Bock C, Rohn G, Ernestus RI, Hoehn M. Metabolic differences between primary and recurrent human brain tumors: a 1H NMR spectroscopic investigation. NMR Biomed 2005;18:371–382.
19. Govindaraju V, Young K, Maudsley AA. Proton NMR chemical shifts and coupling constants for brain metabolites. NMR Biomed 2000;13:129–153.
20. Holmes E, Antti H. Chemometric contributions to the evolution of metabonomics: mathematical solutions to characterising and interpreting complex biological NMR spectra. Analyst 2002;127:1549–1557.
21. Kell DB, Brown M, Davey HM, Dunn WB, Spasic I, Oliver SG. Metabolic footprinting and systems biology: the medium is the message. Nat Rev Microbiol 2005;3:557–565.
22. Piotto M, Bourdonneau M, Furrer J, Bianco A, Raya J, Elbayed K. Destruction of magnetization during TOCSY experiments performed under magic angle spinning: effect of radial B1 inhomogeneities. J Magn Reson 2001;149:114–118.
23. Elbayed K, Dillmann B, Raya J, Piotto M, Engelke F. Field modulation effects induced by sample spinning: application to high-resolution magic angle spinning NMR. J Magn Reson 2005;174:2–26.
24. Davis AL, Keeler J, Laue ED, Moskau D. Experiments for recording pure absorption heteronuclear correlation spectra using pulsed field gradients. J Magn Reson 1992;98:207–216.
25. Fiehn O, Kristal B, van Ommen B, Sumner LW, Sansone SA, Taylor C, Hardy N, Kaddurah-Daouk R. Establishing reporting standards for metabolomic and metabonomic studies: a call for participation. OMICS 2006;10:158–163.
26. Tenenhaus M. La régression PLS. Théorie et pratique. Paris: Technip; 1998.
27. Giammarile F, Cinotti LE, Jouvet A, Ramackers JM, Saint Pierre G, Thiesse P, Jouanneau E, Guyotat J, Pelissou-Guyotat I, Setiey A, Honnorat J, Le Bars D, Frappaz D. High and low grade oligodendrogliomas (ODG): correlation of amino-acid and glucose uptakes using PET and histological classifications. J Neurooncol 2004;68:263–274.
28. Harris AL. Hypoxia—a key regulatory factor in tumour growth. Nat Rev Cancer 2002;2:38–47.
29. Gatenby RA, Gillies RJ. Why do cancers have high aerobic glycolysis? Nat Rev Cancer 2004;4:891–899.
30. Costello LC, Franklin RB. "Why do tumour cells glycolyse?": from glycolysis through citrate to lipogenesis. Mol Cell Biochem 2005;280:1–8.